

ANALYSIS AND COMPARISON OF UNIVERSAL gm-C BIQUAD STRUCTURES

Tomina Fabiola SALAJAN, Iulian CAMPANU,
Raul ONET, Marius NEAG, Marina TOPA
Technical University of Cluj-Napoca
tomina.salajan@bel.utcluj.ro

Abstract: This paper presents a comparative analysis of four multiple-input single-output (MISO) universal gm-C biquads - functional blocks able to implement second-order transfer functions such as low-pass, high-pass, band-pass, band-stop and all-pass without changes to their topology. The analysis focuses on the effects of the parasitic capacitances associated with the unloaded nodes of the biquads - nodes where no capacitance is placed - and the performance of the resulting filters. Performance comparison is based on both analytical analysis and simulation results and considers the orthogonality of the biquads, area and current consumption, how the parasitic capacitances affect the main poles of the transfer function and the capability of a differential implementation.

Keywords: universal biquad, gm-C, parasitic capacitance, transfer function, complex zero, imaginary zero

I. INTRODUCTION

A universal filter is defined as a structure that can implement several transfer functions without needing any change in its structure. So, by simply changing where the input signal is applied or from where the output signal is taken, low-pass (LP), high-pass (HP), band-pass (BP), notch and all-pass (AP) transfer functions can be obtained.

Various solutions can be employed to implement universal biquads [1], [2]. Voltage-mode implementations use operational amplifiers – OA-RC topologies, or linear transconductors – gm-C topologies, while current-mode implementations use current conveyors, CCs, or current feedback operational amplifiers, CFBOAs. Out of these, the gm-C topology is particularly well suited for silicon integration and allows operating at frequencies up to hundreds of MHz. Moreover, the transconductance can be continuously adjusted, thus enabling a precise control of the transfer function parameters. This paper analyses four gm-C universal biquad topologies.

The effect of various nonidealities, like frequency-dependent transconductance, the input and output parasitic capacitances of the transconductors, node parasitic capacitances, and output parasitic conductance, on the universal filters transfer function was derived through equations in [5]. In this paper, a similar analysis is used to compare four of the recently published structures of second-order universal biquads [4]-[7], mainly by taking into account the effect of the parasitic capacitances in the unloaded nodes, i.e. nodes with no connected capacitors.

For the analytical analysis of the biquads, the pole splitting and pole clustering methods described in [3] are

used to approximate the expressions for all the poles in the circuit. The pole splitting method assumes the roots of the analysed polynomial are grouped in distanced regions. If this is not the case for some of the poles, pole clustering will be applied. One of the disadvantages of this method is that a pair of real roots can appear as a pair of complex roots.

Following this short *Introduction* section, the second chapter deals with the *Analysis* of the four chosen universal biquad structures. The circuit schematics are shown, and the location of the parasitic capacitors are identified for each case. The transfer functions are derived for the circuits without parasitic capacitances, then the poles are computed. Next the same procedure is performed considering the parasitic capacitances. Suggestions about sizing and tuning are presented. In third section, the four analysed universal biquads are sized for the same set of requirements. Their transfer functions are obtained through simulations and then their performances are discussed in the *Comparison* section. Also, suggestions for choosing the most suitable universal biquad for a specific application are provided. Lastly, *conclusions* are drawn.

II. gm-C BIQUAD STRUCTURES ANALYSIS II.1. Abuelma'atti Universal Biquad

The biquad presented in Figure 1 [4] employs 7 single-ended gm-cells to form a multiple-inputs single-output (MISO) universal biquad. This biquad can operate in both voltage and current modes, as well as transconductance and transresistance modes. This versatility can prove very useful as it can easily become an interface between circuits

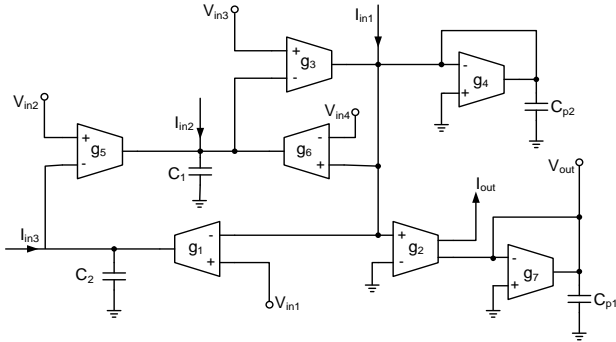


Figure 1: Abuelma'atti universal biquad, with parasitic capacitances C_{p1} and C_{p2} highlighted.

that operate in different modes.

This filter provides five transfer functions, LPF, HPF, BPF, notch and APF, by setting the corresponding values to the voltage and current inputs respectively [4]. The second order voltage transfer function, given in eq. (1), has two complex-conjugated poles.

$$V_{out} = \frac{g_2 g_3}{g_4 g_7} \cdot \frac{s^2 V_{in3} - s \frac{g_5}{C_1} V_{in2} + s \frac{g_6}{C_1} V_{in4} + \frac{g_1 g_5}{C_1 C_2} V_{in1}}{s^2 + s \frac{g_3 g_6}{g_4 C_1} + \frac{g_1 g_3 g_5}{g_4 C_1 C_2}} \quad (1)$$

The transfer function parameters are given in eq. (2):

$$H_0 = \frac{g_2 g_3}{g_4 g_7}; \quad \omega_{0p} = \sqrt{\frac{g_1 g_3 g_5}{g_4 C_1 C_2}}; \quad Q_p = \frac{1}{g_6} \sqrt{\frac{C_1 g_4 g_1 g_5}{C_2 g_3}} \quad (2)$$

$$\omega_{0z} = \sqrt{\frac{g_1 g_5}{C_1 C_2}}; \quad Q_{0z} = \sqrt{\frac{g_1 C_1}{g_5 C_2}}$$

One can notice that the cutoff frequency ω_{0p} can be adjusted through the product $g_1 g_3$ if the ratio g_1/g_3 is kept constant, thus also keeping Q_p constant. Q_p can be orthogonally controlled by modifying g_6 . The gain can also be controlled orthogonally through g_2 and/or g_7 . A possible sizing strategy is to choose $C_1=C_2$, g_1 , g_4 , g_7 and the other circuit elements are found as given in eq. (3).

$$g_5 = \omega_{0z}^2 \frac{C_1 C_2}{g_1}; \quad g_6 = g_5;$$

$$g_3 = \omega_{0p}^2 \frac{g_4 C_1 C_2}{g_1 g_5} = \omega_{0p}^2 \frac{g_4 C_1 C_2}{g_1 \omega_{0z}^2 \frac{C_1 C_2}{g_1}} = g_4 \frac{\omega_{0p}^2}{\omega_{0z}^2}; \quad (3)$$

$$g_2 = H_0 \frac{g_4 g_7}{g_3} = H_0 \frac{g_4 g_7}{g_4 \frac{\omega_{0p}^2}{\omega_{0z}^2}} = H_0 g_7 \frac{\omega_{0z}^2}{\omega_{0p}^2}$$

Two nodes without placed capacitors have been identified in the Abuelma'atti biquad, so the parasitic capacitances present in those nodes are highlighted as C_{p1} and C_{p2} and are used in the following analysis. The denominator of the transfer function becomes of the fourth order, with two extra coefficients: $s^4 \frac{C_{p1} C_{p2}}{g_4 g_7}$ and $s^3 (\frac{C_{p1}}{g_4} + \frac{C_{p2}}{g_7})$. The transfer function poles are obtained using the pole-splitting and pole-clustering algorithms, and their expression is given in eq. (4).

$$p_1 = -\frac{1}{2} \frac{g_3 g_6 C_2 - \sqrt{g_3^2 g_6^2 C_2^2 - 4 g_1 g_3 g_4 g_5 C_1 C_2}}{g_4 C_1 C_2};$$

$$p_2 = -\frac{1}{2} \frac{g_3 g_6 C_2 + \sqrt{g_3^2 g_6^2 C_2^2 - 4 g_1 g_3 g_4 g_5 C_1 C_2}}{g_4 C_1 C_2}; \quad (4)$$

$$p_3 = -\frac{g_4 g_7}{C_{p1} g_7 + C_{p2} g_4}; \quad p_4 = -\frac{C_{p1} g_7 + C_{p2} g_4}{C_{p1} C_{p2}}$$

It becomes clear from eq. (4) that in order to push p_3 and p_4 far above the maximum operating frequency and reduce the impact of the parasitic capacitances, they have to be kept to a minimum, while g_4 and g_7 have to be as large as possible. This condition can be met using the proposed sizing strategy.

II.2. Lee Universal Biquad

The biquad presented in Figure 2 [5] is also a multiple-mode universal filter, as it can operate in voltage-mode, current-mode, transconductance-mode and transresistance mode. It employs two grounded capacitors and five gm-cells with multiple outputs. It has three current/voltage inputs and one current/voltage output, so it is a MISO system. Although the components count is small, so a small on-chip area and power dissipation can be achieved, a major disadvantage of this structure is that it cannot support a fully-differential implementation.

Using this filter, it is possible to obtain five transfer functions, LPF, HPF, BPF, notch and APF, by setting the corresponding values to the voltage and current inputs, respectively [5]. The second order voltage transfer function is given in eq. (5) [5]:

$$V_{out} = \frac{g_3}{g_4} \frac{s^2 V_{in3} - s \frac{g_2}{C_2} V_{in2} + \frac{g_1 g_2}{C_1 C_2} V_{in1}}{s^2 + s \frac{g_3}{C_2} + \frac{g_2 g_3}{C_1 C_2}} \quad (5)$$

The cutoff frequency and the quality factor of this universal biquad are given in eq. (6). These can be orthogonally controlled through g_2 and g_3 by keeping the ratio constant and modifying their product.

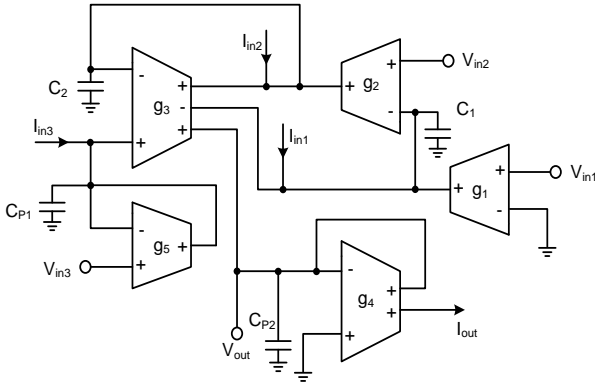


Figure 2: Lee universal biquad, with parasitic capacitances C_{p1} and C_{p2} highlighted.

$$H_0 = \frac{g_3}{g_4}; \omega_{0p} = \sqrt{\frac{g_2 g_3}{C_1 C_2}}; Q_p = \sqrt{\frac{C_2 g_2}{C_1 g_3}}; \quad (6)$$

$$\omega_{0z} = \sqrt{\frac{g_1 g_2}{C_1 C_2}}; Q_z = \sqrt{\frac{g_1 C_2}{g_2 C_1}}$$

A possible sizing strategy is to choose C_1 , g_3 and g_5 . It results that:

$$C_2 = \frac{\omega_{0z}}{\omega_{0p}} C_1; g_2 = \omega_{0p}^2 \frac{C_1 C_2}{g_3} = Q_p^2 g_3 \frac{C_1}{C_2}; \quad (7)$$

$$g_4 = \frac{g_3}{H_0}; g_1 = \omega_{0z}^2 \frac{C_1 C_2}{g_2} = Q_z^2 g_2 \frac{C_1}{C_2}$$

Lee biquad has two nodes without placed capacitances, where C_{p1} and C_{p2} are considered for the following analysis. It results a 4th order transfer function, with coefficients containing C_{p1} and C_{p2} found in both the numerator and denominator, affecting the second order transfer function parameters. The expressions of the poles of the third order denominator were derived using the pole-splitting and pole-clustering algorithms. Their dependence on the circuit elements is given in eq. (8).

$$p_1 = f\left(g_2, g_3, C_1, C_2, \frac{C_{p1}}{g_5}, \frac{C_{p2}}{g_4}\right);$$

$$p_2 = f\left(g_2, g_3, C_1, C_2, \frac{C_{p1}}{g_5}, \frac{C_{p2}}{g_4}\right);$$

$$p_3 = f\left(g_2, g_3, C_1, C_2, \frac{C_{p1}}{g_5}, \frac{C_{p2}}{g_4}\right); \quad (8)$$

$$p_4 = f\left(g_3, C_2, \frac{C_{p1}}{g_5}, \frac{C_{p2}}{g_4}\right).$$

In order to push p_3 and p_4 far above the maximum operating frequency, one needs to size g_4 and g_5 as large as possible – similar to the Abuelma'atti universal biquad.

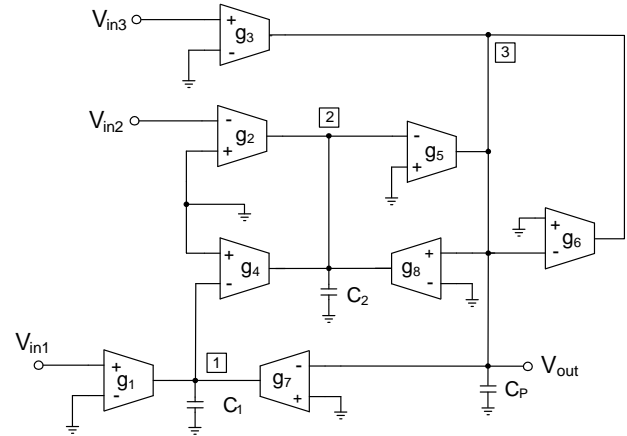


Figure 3: Neag 1 universal biquad, with parasitic capacitance C_p highlighted.

II.3. Neag 1 Universal Biquad

The biquad presented in Figure 3 [6] contains eight gm-cells with a single output and two grounded capacitors. It has three inputs and one output, so it is a MISO type universal filter. Filters with complex zeroes, pure imaginary zeros, LPF, HPF, BPF and APF can be obtained by setting the corresponding values to the input voltages, as shown in [6]. The voltage transfer function is given in eq. (9).

$$V_{out}(s) = \frac{g_3}{g_6} \frac{V_{in3} s^2 + V_{in2} s \frac{g_2 g_5}{g_3 C_2} + V_{in1} \frac{g_1 g_4 g_5}{g_3 C_1 C_2}}{s^2 + s \frac{g_5 g_8}{g_6 C_2} + \frac{g_4 g_5 g_7}{g_6 C_1 C_2}} \quad (9)$$

The expressions of the canonical parameters - H_0 , ω_p , ω_z , Q_p and Q_z - result as follows:

$$H_0 = \frac{g_3}{g_6}; \omega_p = \sqrt{\frac{g_4 g_5 g_7}{g_6 C_1 C_2}}; \omega_z = \sqrt{\frac{g_1 g_4 g_5}{g_3 C_1 C_2}}; \quad (10)$$

$$\frac{1}{Q_p} = g_8 \sqrt{\frac{g_5}{g_4 g_6 g_7} \frac{C_1}{C_2}}; \frac{1}{Q_z} = g_2 \sqrt{\frac{g_5}{g_1 g_3 g_4} \frac{C_1}{C_2}}$$

These expressions highlight the following transfer function parameter – controlling element pairs: (ω_z and g_1), (Q_z and g_2), (ω_p and g_4), (Q_p and g_8) and (H_0 and g_3). A possible sizing strategy is to choose the values for the following circuit elements: $C_1=C_2$, g_1 , g_3 and g_4 . The values for the rest of the circuit elements are obtained as follows:

$$g_6 = \frac{g_3}{H_0}; g_5 = \omega_z^2 \frac{C_1^2 g_3}{g_1 g_4}; g_7 = \omega_p^2 \frac{C_1^2 g_6}{g_4 g_5};$$

$$g_8 = \frac{1}{Q_p} \sqrt{\frac{g_4 g_6 g_7}{g_5}}; g_2 = \frac{1}{Q_z} \sqrt{\frac{g_1 g_3 g_4}{g_5}}. \quad (11)$$

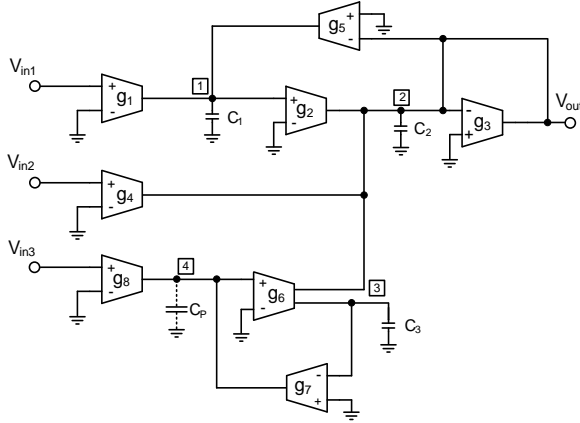


Figure 4: Neag 2 universal biquad, with parasitic capacitance C_p highlighted.

When the parasitic capacitor, C_p , in the unloaded node is considered, the voltage transfer characteristic becomes of the third order, with one extra coefficient in the denominator: $s^3/C_p g_6$. The expressions for the poles were derived using the pole-splitting and pole-clustering algorithms, and are given in eq. (12).

$$p_1 = -\frac{1}{2} \frac{g_5 g_8 + \sqrt{g_5^2 g_8^2 - 4 \frac{g_4 g_5 g_6 g_7 C_2}{C_1}}}{g_6 C_2};$$

$$p_2 = -\frac{1}{2} \frac{g_5 g_8 - \sqrt{g_5^2 g_8^2 - 4 \frac{g_4 g_5 g_6 g_7 C_2}{C_1}}}{g_6 C_2}; \quad (12)$$

$$p_3 = -\frac{g_6}{C_p}.$$

In order to reduce the effect of the parasitic capacitance, one has to increase the g_6/C_p ratio up to at least 2 times greater than the maximum operating frequency, such that the associated pole is taken to the high frequency range, where it will not affect the biquad behavior.

II.4. Neag 2 Universal Biquad

The universal biquad presented in Figure 4 [7] implements, with minimum adjustments, a large range of second order filters, from the usual low-pass and band-pass to transfer functions with complex and fully-imaginary zeroes. This biquad utilizes eight gm-cells and three grounded capacitors. It has only one unloaded node, marked as node 4 in Figure 4, together with the node parasitic capacitance, C_p . The expression of the output voltage, when C_p is neglected, is given in eq. (13) [7].

$$V_{out}(s) = \frac{g_8 C_3}{g_7 C_2} \frac{V_{in3} s^2 + V_{in2} s \frac{g_4 g_7}{g_8 C_3} + V_{in1} \frac{g_1 g_2 g_7}{g_8 C_1 C_3}}{s^2 + s \frac{g_3}{C_2} + \frac{g_2 g_5}{C_1 C_2}} \quad (13)$$

Apparently, the effect of C_p over the transfer function is more significant than in case of the other analysed biquads and cannot be neglected. But the capacitance C_p appears in parallel with the inductance L_{ech} synthesized by the gyrator implemented by g_6 and g_7 , connected in antiparallel, and C_3 , as shown in Figure 4. The equivalent impedance seen in node 4 when considering the parasitic capacitance is very close to the one obtained when neglecting C_p , up to the resonance frequency of the $L_{ech}-C_p$ network,

$$f_{res} = \frac{1}{2\pi} \sqrt{\frac{g_6 g_7}{C_3 C_p}}.$$

Thus, the effect of the parasitic capacitance C_p on the biquad transfer function can be minimized by setting the resonance frequency, f_{res} , well above the maximum operating frequency.

The expressions of the transfer function canonical parameters, H_0 , ω_p , ω_z , Q_p and Q_z , are given in eq. (14).

$$H_0 = \frac{g_8 C_3}{g_7 C_2}; \omega_p = \sqrt{\frac{g_2 g_5}{C_1 C_2}}; Q_p = \frac{1}{g_3} \sqrt{g_2 g_5 \frac{C_2}{C_1}};$$

$$\omega_z = \sqrt{\frac{g_1 g_2 g_7}{g_8 C_1 C_3}}; Q_z = \frac{1}{g_4} \sqrt{\frac{g_1 g_2 g_8 C_3}{g_7 C_1}}. \quad (14)$$

These expressions highlight the following transfer function parameter – controlling element pairs: (ω_z and g_1), (Q_z and g_4), (ω_p and g_5), (Q_p and g_3) and (H_0 and g_7). A possible sizing strategy is to choose the values for the following circuit elements: C_1 , C_2 , C_3 , g_1 , g_7 , f_{res} and to estimate the value of C_p . The values for the rest of the circuit elements are obtained as follows:

$$g_6 = (2\pi \cdot f_{res})^2 \frac{C_3 C_p}{g_7}; g_8 = H_0 \frac{g_7 C_2}{C_3};$$

$$g_2 = \omega_z^2 \frac{g_8 C_1 C_3}{g_1 g_7}; g_5 = \omega_p^2 \frac{C_1 C_2}{g_2}; \quad (15)$$

$$g_3 = \frac{1}{Q_p} \sqrt{g_2 g_5 \frac{C_2}{C_1}}; g_4 = \frac{1}{Q_z} \sqrt{\frac{g_1 g_2 g_8 C_3}{g_7 C_1}}.$$

III. DESIGN EXAMPLE

The four universal biquad structures are all sized in order to meet the same set of specifications: $f_p=f_z=10$ MHz, $Q_p=Q_z=1$ and $H_0=1$, for ensuring a fair comparison. The circuit elements, derived using the sizing strategies discussed in the previous section, are given in Table 1. Although several transfer functions can be obtained, only the high-pass transfer characteristic is presented here to illustrate the performances of the analysed biquads.

The biquads were implemented using a simple transconductor model with a very large output resistance, $R_{out}=1G\Omega$. Figure 5 presents, with dashed lines, the four analysed biquads frequency characteristics when the parasitic capacitances are neglected, and, with continuous lines, the same frequency characteristics when parasitic capacitances of 100 fF were placed in each unloaded node.

Table 1: Values of the circuit elements of the 4 analysed biquads.

Circuit elements	Abuelma'atti	Lee	Neag 1	Neag 2
g_1 [uS]	727	1070	551	551
g_2 [uS]	1420	369	1100	716
g_3 [uS]	1420	1070	1250	628
g_4 [uS]	1420	1070	1250	628
g_5 [uS]	543	1420	716	551
g_6 [uS]	543	-	1250	200
g_7 [uS]	1420	-	551	902
g_8 [uS]	-	-	1100	902
C_1 [pF]	10	10	10	10
C_2 [pF]	10	10	10	10
C_3 [pF]	-	-	-	10
C_p [pF]	-	-	0.1	0.1
C_{p1} [pF]	0.1	0.1	-	-
C_{p2} [pF]	0.1	0.1	-	-

The effect of the parasitic capacitances can be noticed starting from frequencies above 1 GHz, where the extra poles introduce attenuation.

The expressions of the poles caused by the parasitic capacitances, derived in the previous section, are validated through simulations: the positions of the poles are computed using the derived formulae and compared with the values obtained using a ‘‘Pole-Zero’’ simulation performed in Cadence Virtuoso environment. Table 2 shows that the values obtained analytically and those obtained from simulation are in very good agreement.

IV. COMPARISON OF THE ANALYSED BIQUAD STRUCTURES

The four presented universal biquad structures are compared by considering various criteria, as follows.

Neag 2 biquad uses the largest number of gm-cells, so it has larger die size and power consumption compared to Abuelma'atti, Lee and Neag 1 biquads, which all use the

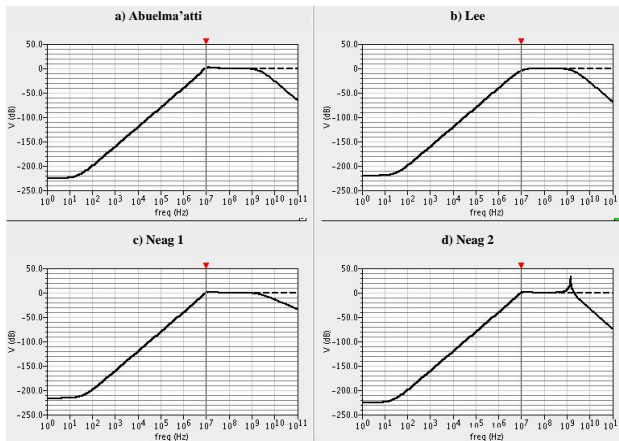


Figure 5: a) Abuelma'atti, b) Lee, c) Neag1 and d) Neag2 universal biquad high-pass transfer characteristics: without parasitic caps - dashed line; with placed parasitic caps of 100fF at the unloaded nodes - continuous line).

Table 2: Comparison between the computed values (c) of the filters' poles and the ones obtained using simulations (s).

Poles		p1 [MHz]		p2 [MHz]		p3 [GHz]	p4 [GHz]
		real	im	real	im	real	real
Abuelma'atti	c	4.32	-9.02	4.32	9.02	1.13	4.52
	s	4.29	-9	4.29	9	2.26	2.27
Lee	c	8.4	-5.22	8.4	5.22	0.984	3.98
	s	8.51	-5.24	8.51	5.24	1.7	2.26
Neag 1	c	5	-8.66	5	8.66	1.99	-
	s	5	-8.67	5	8.67	1.979	-
Neag 2	c	5	-8.66	5	8.66	-	-
	s	4.99	-8.65	4.99	8.65	-	-

same number of gm-cells.

Abuelma'atti and Lee biquads have two unloaded nodes, increasing the number of poles, when considering the parasitic capacitances effect. Still, the main poles, p_1 and p_2 , are affected by the parasitic capacitances only in the case of Lee biquad. In comparison, Neag 1 and Neag 2 biquads have only one unloaded node, thus, Neag 1 and Neag 2 biquads present a smaller sensitivity to parasitic capacitances.

By analyzing the circuit elements values presented in Table 1, it can be seen that Neag 1 biquad has the lowest g_m spread, defined as the ratio between the minimum and maximum g_m values used in the biquad.

When considering the tunability criterion, neither of the four analysed biquads is orthogonal, but various strategies can be found for each biquad in order to vary the gain or the cutoff frequency and the corresponding quality factor through parameter-controlling element pairs, as demonstrated in the previous chapter.

Finally, only Neag 1 and Neag 2 structures can be extended to implement fully differential filters, which allows reducing common-mode noise and disturbances and increases linearity.

Table 3 summarizes the comparison between the four universal biquads and it can be used as a guideline for choosing the most suitable biquad for a given set of specifications.

V. CONCLUSIONS

Four recently published gm-C universal biquad structures were analysed in this paper. Their transfer functions were derived when considering the parasitic capacitances from the unloaded nodes. The analytical expression of the poles was approximated using the pole-splitting and pole-clustering algorithms. For each analysed structure, a sizing strategy that allows minimizing the effects of the parasitical capacitances was proposed.

The analysis was validated with a sizing example, where a simple transconductor model was used. Further research will also consider the effect of real gm-cells.

The analysed structures were compared, by taking into account various criteria like: number of gm-cells, number of unloaded nodes, the effect of the parasitic capacitances on the biquad performances, the orthogonality and the capability of a fully differential implementation. Of course,

Table 3: Comparison between the four presented universal biquad structures.

	Abuel ma'atti	Lee	Neag 1	Neag 2
No. of g_m cells (outputs)	8	8	8	9
No. of unloaded nodes	2	2	1	1
No. of poles	4	4	3	2
C_{par} affects p_1, p_2	No	Yes	No	No
Allows differential implementation	No	No	Yes	Yes
G_m spread	1:2.6	1:2.9	1:2.26	1:4.51

no clear winner could be designated, but depending on the requirements of the system in which the universal biquad is to be used, suggestions were given to help the designer make the most suitable choice.

REFERENCES

- [1] M. Neag, "Sisteme cu circuite integrate analogice", *Mediamira*, 2008.
- [2] Deliyannis, T., Y. Sun, JK. Fidler, "Continuous time active filter design", *CRC Press*, USA, 1999.
- [3] Marina Dana Țopa, "Analiza simbolică a circuitelor electronice", *Casa Cărții de Știință*, 1998.
- [4] Abuelma'atti, Muhammad Taher, and Abdulwahab Bentrchia. "A novel mixed-mode OTA-C universal filter", *International Journal of Electronics* 92.7, 2005: pp. 375-383.
- [5] Lee, Chen-Nong. "Multiple-mode OTA-C universal biquad filters", *Circuits, Systems and Signal Processing* 29.2, 2010: pp. 263-274.
- [6] Neag, Marius, Liviu Nedelea, Marina Țopa, Lelia Feștilă, "A New OTA-C Electronically Tunable Orthogonal Universal Biquad", *Proceedings of the International ProRISC*, 23-24 November, 2006, Veldhoven, Olanda, pp. 61-66.
- [7] Neag, Marius, Raul Oneț, and Marina Țopa. "A new OTA-C universal biquad resonates out the main parasitic capacitance." *Circuit Theory and Design*, 2009. ECCTD 2009. European Conference on. IEEE, 2009, pp. 124-128.